

Local Pre-processing for Node Classification in Networks Application in Protein-Protein Interaction

Christopher E. Foley^{1,2}, Sana Al Azwari¹, Mark Dufton²,
Isla Ross¹, and John N. Wilson¹

¹ Department of Computer & Information Sciences

² Department of Pure & Applied Chemistry
University of Strathclyde, Glasgow, UK

Abstract. Network modelling provides an increasingly popular conceptualisation in a wide range of domains, including the analysis of protein structure. Typical approaches to analysis model parameter values at nodes within the network. The spherical locality around a node provides a microenvironment that can be used to characterise an area of a network rather than a particular point within it. Microenvironments that centre on the nodes in a protein chain can be used to quantify parameters that are related to protein functionality. They also permit particular patterns of such parameters in node-centred microenvironments to be used to locate sites of particular interest. This paper evaluates an approach to index generation that seeks to rapidly construct microenvironment data. The results show that index generation performs best when the radius of microenvironments matches the granularity of the index. Results are presented to show that such microenvironments improve the utility of protein chain parameters in classifying the structural characteristics of nodes using both support vector machines and neural networks.

1 Introduction

Connected topologies have emerged as a productive way of modelling a wide variety of social, technical and biological systems. Among other domains, the paradigm has been used to characterise social networks [1], protein structures and interactions [3], genetic control [20], market economies [21] and human and machine communication [2]. The power and flexibility of the network concept is highly adaptable as a basis for explaining the overall behaviour of a system but an emerging theme of such modelling is the potential for identifying specific regions in a network that are of particular interest. Such hotspots might represent localised communities in social networks [1] or periods of excessive workload in computer networks [28]. In the remainder of this discussion, we focus particularly on networks that represent protein structural topology and hotspots that characterise points of interaction between proteins. However the novel concept presented here (i.e. the use of localisation to enhance the hotspot detection process) has potential for application in other domains modelled by networks.

The physicochemical properties of proteins provide useful information that results in the identification of new drug targets. Virtual screening offers a methodology for processing entire data collections such as the Protein Data Bank (PDB)[9] with the aim of identifying useful new drug leads. However, it is important to design the screening process in such a way that the maximum benefit is extracted from the data available. An understanding of the structure of proteins and their data representation can guide the design of effective screening methodologies.

A protein is a chain (or combination of chains) of amino acid residues. The chain consists of a backbone that includes the α -carbon atom from each residue in the chain. Protein structures have been modelled as networks with the residues representing the nodes of the graph and edges representing residue interactions [3]. It is also possible to conceptualise nodes as discrete atoms in a protein structure with the edges representing inter-atom factors such as distance. The microenvironment that surrounds each α -carbon is characterised by all the atoms in the network that fall within a defined sphere (Figure 1). Where multiple chains are present, interactions may take place between the residues in different chains. Such protein-protein interaction sites contribute to the function of a protein. Consequently, prediction of the localities of interactions between proteins can be a guide to function prediction for a particular site [11]. Characterising the locality (rather than a point) in a protein structure can be addressed by evaluating microenvironments rather than the specific values associated with particular locations.

Proteins are made from the polymerisation of amino acids into a linear chain that is folded into a three dimensional (3D) structure. The folding pattern brings the functional parts of the protein together and adjusts its configuration in response to binding interactions. The positions of the atoms are determined by processes such as X-Ray Crystallography. Over 70000 3D protein structures are available from the PDB.

A microenvironment is the localised three dimensional spherical neighbourhood surrounding a particular node within a network. In this case the nodes are represented by the α -carbons within a protein structure and the edges by the distance between neighbouring α -carbons. Each microenvironment encloses a variable number of nodes in the network, depending on the radius of the sphere. Figure 2(a) shows the location of amino acids that contribute to the protein-protein interaction site of 1HLU chain A (Bovine Beta-Actin-Profilin). Choosing one particular amino acid (in the case of Figure 2(a) the amino acid at position 89 in the chain is chosen) and defining microenvironments of radius 4Å, 10Å and 20Å causes an increasing number of neighbouring amino acids to be included in the microenvironment cluster as indicated in Figures 2(b) to 2(d). The use of microenvironments as a basis for data mining requires an efficient means of identifying data instances that are within a certain distance of each other. As part of an effort to predict druggable sites on a protein (that is discrete areas where a small drug molecule can regulate the action of the protein) temperature factor can be used as an estimate of flexibility [32]. Protein analysis

reveals the variation in 3D location of atoms in a protein as the temperature factor (B factor) parameter. Proteins are not rigid structures. In fact, much of the functionality of a protein depends on small positional adjustments. Temperature factor gives an indication of the likelihood of these adjustments taking place at each atom in the protein structure. The mean temperature factor of all the atoms enclosed in a microenvironment provides a value for this parameter that is based on the flexibility of the locality surrounding a single α -carbon in a chain rather than the flexibility of a single point. This is a consequence of the dependence of the protein topology on the plasticity of the local structure. Since any individual residue may be part of several spheres, pre-processing nodes in the structural network provides an estimate of the protein's behaviour in the surrounding area rather than behaviour at the point represented by each node. This is useful because the activity of a protein is influenced by the general topology rather than point-by-point parameter values, that is in the general context of networks, the structures behave as communities rather than a set of discrete nodes. The temperature factor of a particular residue represents only the flexibility at a specific node in the protein structure network. Other residue parameters such as hydrophobicity[11] (the extent to which the residue repels water) can be evaluated for microenvironments using a similar approach and together these parameters can be used to classify the residues in a chain on the basis of their likely contribution to protein-protein binding sites [10].

A range of processes are available for establishing classifications in datasets, however support vector machines (SVM) and neural networks (NN) typically span the range of prediction accuracies of such methods [10]. An SVM [14]

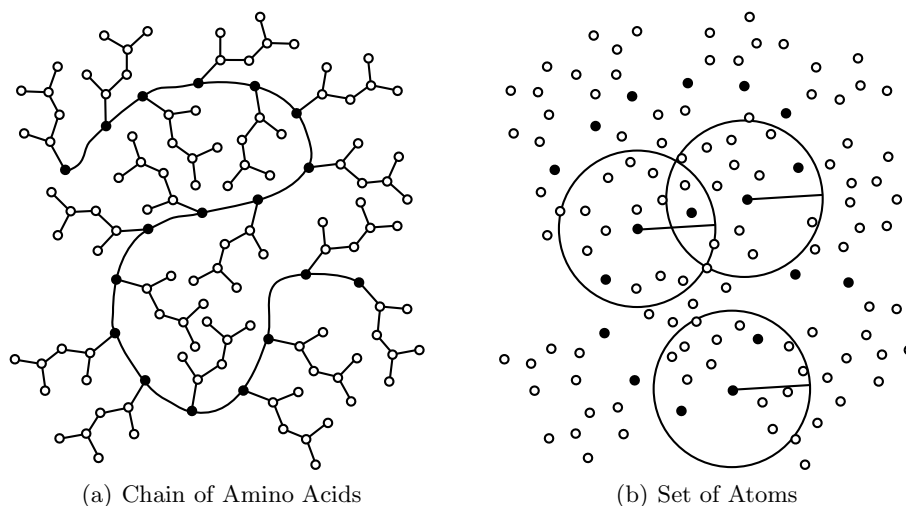


Fig. 1. Simplified representations of a protein. α -carbons are black and the side chain atoms are hollow. Microenvironment spheres are defined around each of the α -carbons (three are shown).

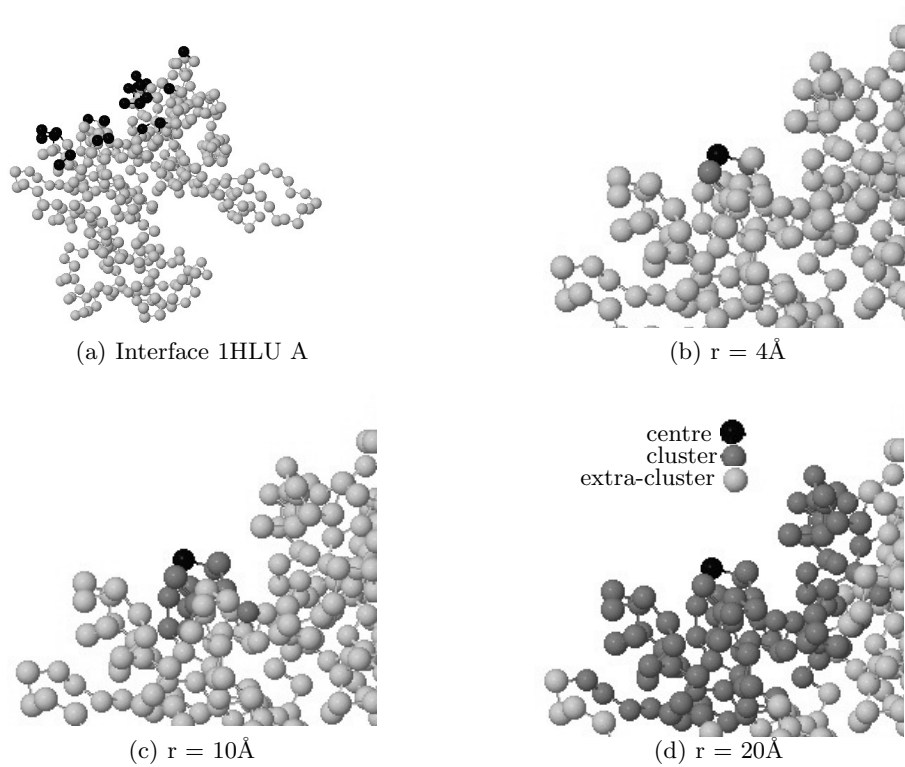


Fig. 2. Amino acid residues clustered in the spheres of varying radii surrounding a single residue centre in the protein-protein interface

is a supervised learning mechanism that generates a hyperplane separating data in a training set. SVMs have been used in bioinformatic research to generate optimal classifications of sites on protein chains [13]. Artificial neural networks represent an alternative approach to classifying input data. They provide a means of deriving a functional model to separate classes in the input data. As with SVMs, NNs are able to classify non-linear data [33]. By training SVMs and NNs with sets of appropriate data, the likely positions of protein-protein interaction sites in a protein chain can be distinguished [24].

There are many possible microenvironment configurations that might be useful in classification nodes within the network. It is not feasible to pre-compute all the possible combinations for any extensive network. Generating microenvironments on-the-fly provides sufficient flexibility and at the same time can support rapid exploration of data. Three dimensional (3D) grid methods have long been known to provide a basis for accelerating the performance of processing spatial data [23]. However in the scenario of varying the level of abstraction of microenvironment data the most appropriate dimensions for box indexes are uncertain.

The contribution of the work described in this paper is to identify the best way of generating an on-the-fly index for the rapid association of nodes within a network. This methodology is then used to demonstrate that the assembly of clustered data makes a significant contribution to predicting hotspots in protein structure networks. In turn, this introduces the general approach of network analysis using localised topological summaries. The rest of the paper is organised as follows: Section 2 establishes the context of related approaches. Section 3 describes index generation and its use in the microenvironment assembly algorithm and presents the experimental work, the results of which are set out in Section 4. The paper concludes with an evaluation of the results and the potential for further work in Sections 5 and 6.

2 Related Work

Improvements in the performance of processing geometric data can be achieved by using specialised data structures. Scenes can be represented in hierarchical trees of bounding volumes [22]. *kd*-trees are a common structure [8] and their traversal allows intersections to be calculated or distances to be measured. When working with point data, Voronoi diagrams [5] can be used to divide the n -dimensional space into sectors around each point. Using this approach, the entire space within each sector is closer to its parent point than to any other point. This is useful for queries that determine nearest neighbours. In applying these principles to processing molecular data, early recognition of the power of quantising the space of individual molecules came from Leventhal [23]. This approach was further contextualised by Bentley [7] who assumed a quantisation based on search radius. The approach described in the current work explores the assumption that the optimum cell size of the quantisation is the same as search radius. Establishing the optimal approach is an essential step in providing a suitably efficient method of microenvironment assembly.

Residue interaction graphs have been used to characterise protein structures [3] with a view to classifying active sites. Hotspots in both social networks and networks representing protein structures have been found to play a key part in the development and persistence of structural aggregations in their various domains [15]. Network analysis tools have been identified as having considerable potential for identifying targets for drug development [18]. Fixed size microenvironments have been used as a basis for *k*-means clustering with a view to exploring protein structure [29]. This approach has also been successful in identifying calcium binding sites [6]. The prediction of protein-protein interaction sites has been explored by using combinations of attributes and SVM classifiers [30,11,35]. Typically these lead to prediction accuracy in the region of 60%-70%. Tuning the algorithm by manipulating nearest-neighbour selection produces a prediction accuracy of 73% [31]. Neural networks have also been used to predict protein-protein interaction sites from combinations of physicochemical parameters [17] and are reported to return accuracy in the region of 70%-72%. The use of microenvironments has been found to provide a basis of screening protein data for the presence of allosterically active sites [12].

The novel idea presented here is that pre-processing network data by the construction of parameter aggregates within microenvironments improves the ability to identify hotspot nodes. This contrasts with previous research that focuses on point parameter data. The effectiveness of this approach is demonstrated using both SVM and NN classifiers in the prediction of protein-protein interface sites.

3 Prediction Model

Microenvironment assembly determines the atoms that lie inside the sphere that is centred on each α -carbon in a protein chain. The simple approach of calculating the Euclidean distance between all residue/atom pairs is inefficient in a network that may consist of thousands of nodes. Cell partitioning [7] is used to pre-organise data so that only nearby atoms are considered as candidates during microenvironment assembly. Generation of the cell index is carried out on-the-fly having previously established the overall maxima and minima of spatial coordinates in the collection of protein structures and this is used to produce a 3D grid. The coordinates of each atom associate it with a particular cell in this grid. The index identifies a candidate set of atoms that can be formed from the surrounding cells, immediately ruling out distant atoms from consideration. Only atoms within a reasonable distance of the sphere centre become candidates. The distances between the candidates and the sphere centre are calculated and the appropriate atoms included in the sphere. The index can be tuned by altering the size of the 3D cells and Figure 3 shows how the candidate set is narrowed down by choosing only the cells that intersect with the sphere. Figure 4 gives a formal description of the index generation algorithm. Given the importance of this step in on-the-fly assembly of microenvironments, it is necessary to assess whether the optimal cell edge length is the same as radius size or whether a sub-multiple (L/n) of radius size would be more appropriate.

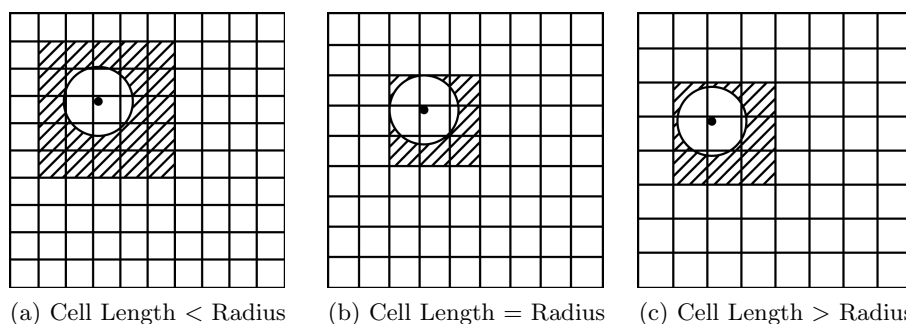


Fig. 3. The relationship between sphere radius and cell length. All of the nearby boxes that intersect with the sphere (or any sphere centred in the same box) are highlighted, and all the atoms from these boxes are candidates for inclusion in the sphere.

```

1: Create a 3D array of cells encompassing all elements in the PDB.
2: for each atom in the chain do
3:   Determine which cell this atom belongs in.
4:   Place a reference to the atom in this cell.
5: for each sphere centre in the chain do
6:   Create an empty sphere.
7:   Determine which cell this sphere centres in.
8:   calculate the length of the shaded area by
9:    $2 \times \lceil \frac{\text{sphere radius}}{\text{box length}} \rceil + 1$ 
10:  for each cell in the shaded area do
11:    for each atom in the cell do
12:      distance =  $\sqrt{\Delta x^2 + \Delta y^2 + \Delta z^2}$ 
13:      if distance < sphere radius then
14:        add this atom centre to the sphere

```

Fig. 4. 3D grid atom allocation algorithm

At one extreme, a single large cell will place all the atoms together, effectively removing any benefit from the index. At the other end of the spectrum, if the cell size is too small each atom will have its own box, negating the advantage. Figure 3 suggests that choosing a cell size that matches the sphere radius constrains the candidate space but that sub-multiples ($L/2$, $L/3$ etc.) might be more effective. A cell length equal to the microenvironment radius maximally constrains the candidate space volume for the smallest number of candidate cells. This volume can be constrained further by using a greater number of smaller cells. Adding another layer of cells reduces the optimum cell size to $L/2$. A further layer reduces it to $L/3$ and cell lengths for these volume minima can be generalised to L/n .

Experimental work was carried out to evaluate the optimal approach to indexing Protein Data Bank (PDB) data [9] with a view to rapid assembly of microenvironments. A second set of experiments evaluates the effect of physico-chemical parameter variation on the detection of hotspots within protein network structures.

3.1 Index Configuration

Experiments were run to configure the 3D grid index in the context of the collected data structures from the PDB. Microenvironments were then assembled using varied sphere radii and protein sizes in order to allow a comparison. The experiments were conducted on a 3 GHz Intel Pentium 4 processor with 1 GB RAM, running Zenwalk Linux 6.2. The algorithms were implemented in Java 6.

To obtain a representative test dataset, the protein chains present in the PDB were divided into groups by chain length (1–50 residues in the first group, 51–100 in the second, etc.) and one chain was chosen at random from each group. The final dataset is shown in Table 1.

Table 1. Set of protein chains used for benchmarking the index algorithms

ID	Ch.	Len	ID	Ch.	Len	ID	Ch.	Len	ID	Ch.	Len
1D9M	A	18	1AZP	A	66	2I8T	B	149	2IX3	B	972
1BGL	F	1021	3DEE	A	197	1J2Q	B	223	2QFQ	C	296
2QN1	A	813	2VC9	A	882	1MIQ	B	327	2OF6	B	400
1JRP	G	450	1UYT	A	681	1N7O	A	721	2HLD	S	480
1ZPU	E	529	1EFK	A	553	2PPB	M	1119	1WZ2	B	948
2AHX	B	615	1JRP	B	760						

The performance evaluation of microenvironment assembly was carried out by repeating the algorithm 1000 times. In order to make sure the compiled and optimised execution was measured, the 1000 measurements were repeated until two consecutive measurements were within 10% of each other. To prevent the benchmarked code being optimised out by the compiler, a summation of the sphere results was calculated and output to the console after the time measurements were complete. To determine the best cell size, the protein size was kept constant. Chain E from 1ZPU was chosen since it is in the middle of the range of chain length, which fixed the number of residues at 529.

An index using cells that are too small will take a long time to create while very large cells will approach $O(n^2)$ in terms of microenvironment assembly performance. Somewhere between these two extremes must lie the maximum efficiency. The experiment was run at sphere radii of 4, 5, 6, 7, 8, 9 and 10Å. For each sphere size, the cell size was varied from 4 Å to 20 Å in steps of 1Å. The best cell size was deduced from the above experiments and used to benchmark the cell index at sphere radii of 4, 5, 6, 7, 8, 9 and 10Å for each chain length in the dataset.

3.2 Aggregating Parameter Values

Having established the optimal approach to microenvironment assembly, experiments were conducted to examine the effect of the approach on the classification of nodes within the protein structural network. In this case, the intention was to identify hotspot nodes representing those residues that take part in protein-protein interactions. Figure 5 illustrates the basis of this approach. In this case, temperature factor is shown for each position in a sample chain (1HLU chain A). The sites of the protein-protein interface are indicated and can be seen to be distributed over peaks and troughs when using a 0Å sphere (i.e point data). In the case of the 40Å dataset, the protein-protein interaction sites have coalesced in troughs in the distribution. This suggests that particular features of the temperature factor distribution are evident at some microenvironment radii but not at others. These variations in parameter distributions are of use in classifying nodes in the network structure of residues.

Table 2. Sample dataset used for benchmarking the microenvironments

ID	Chs.	ID	Chs.	ID	Chs.	ID	Chs.	ID	Chs.	ID	Chs.	ID	Chs.		
1AHWB	C	1AVG	H I	1AY7	A B	1AZS	C B	1B6C	A B	1B7Y	A B	1BDJ	A B	1BI7	A B
1BMQ	A B	1BP3	A B	1BVK	A C	1BVN	P T	1D4V	A B	1DAN	L U	1EBD	A C	1EFU	A B
1ETH	A B	1GFW	A B	1GLA	F G	1GOT	B G	1HJA	B I	1HLU	A P	1IRA	X Y	1KKL	A H
1LOY	A B	1NOC	A B	1PDK	A B	1QBK	B C	1SMP	A I	1STF	E I	1UDI	E I	1UEA	A B
1VAD	A B	1ZBD	A B	2PCC	A B	3EZE	A B	7CEI	A B						

Table 3. Dataset parameters

Parameter	Characteristic
Temperature factor (<i>B</i> -factor)	The flexibility of the protein at a particular atom.
Druggability	The likelihood of targetting by a drug-like molecule.
Hydrophobicity	The extent to which the residue repels water.
Total atomic weight	The local size at a node.
Residue number	Position in the protein chain.

Table 4. Dataset size

Parameter	Count
Total residues	24526
Exposed residues	7977
Interface residues	4104

To verify this assumption, a set of chain pairs with prior established protein-protein interaction sites was identified [4]. This set was further refined by removing chains containing multiple models (i.e. where variations in the configuration of the protein were possible) and those identified as containing significant redundancy [24]. Lastly, chains that had no matching pair subsequent to these steps were also removed. Following this process, the sample set consisted of those chain pairs shown in Table 2.

The residues in each chain of this set were then classified on the basis of their proximity to residues in the complementary chain. The occurrence of two α -carbons from complementary chains within a range of 12Å was taken as an indication that the respective locations of these residues represented a protein-protein interaction site [24]. The α -carbons in each chain were also classified on the basis of their accessible surface area (ASA) [19]. Surface residues were taken to be those with an ASA more than 20% of the surface area. The dataset chosen is summarised in Table 4.

A set of parameters indicated by previous work [16,26] was then derived for each surface residue in each chain. The parameters represent orthogonal characteristics of nodes within the network as shown in Table 3. Microenvironments of radii 0Å to 50Å were used to produce a mean value for each of these parameters for each node using the approach explained in subsection 3.1. For temperature factor and total atomic weight, each atom in the microenvironment provides a contribution to this mean. For other parameters used, each residue included in the locality provides a contribution.

This approach generated a vector of values that were used with both neural net (NN) and support vector machine (SVM) classifiers. Non-overlapping training and test sets were generated by assigning alternate microenvironments to each of these two sets. The LIBSVM package [13] was used to develop a support vector machine classification model using the training set of residues. In the course of generating the classification, cross-validation was carried out within the training

set. A non-linear function provided the best separation for distinguishing protein-protein interaction sites using an SVM. Neural net classifiers were generated and tested using Matlab [25] and the same training and test sets as were used to generate the SVM classifications. As with the SVM classifiers, cross-validation was carried out within the training set during generation of the NN classifiers.

4 Experimental Results

The performance of microenvironment assembly based on a properly configured cell index is shown in Figure 6. The maximum number of amino residues in a single chain in the PDB is 4128, suggesting that index generation will be around 0.6 seconds in the worst case.

It can be seen from Figure 7, that the most efficient cell size is equal to the sphere radius. As the cell size increases from this global minimum, the time for the algorithm to run increases steadily. This is consistent with the larger cells holding progressively more atoms and therefore requiring more distance calculations. As the cell size decreases from the global minimum, the trend is for the time to increase. This is because more cells are required and their creation becomes the most time-intensive step. However Figure 7 also shows local minima at half the optimum cell size. Consider determining the sphere at a 7\AA radius. When the cell size is also 7\AA , the candidate list is drawn from the central cell and all of the surrounding cells. If the cell size is decreased to 6\AA we still have to check the central cell and the surrounding ones. However, now the range of the sphere can include atoms up to two cells away. If we go below 3.5\AA (half the optimum box size), we have to consider atoms three cells away. One could expect another local minimum at 1.75\AA , another at half this, and so on. The results from the optimum configuration are shown in Figure 8. Microenvironment assembly using the 3D grid index differs in that the speed varies with the sphere size.

The impact of changing the radius of the sphere on the identification of hotspot nodes in the context of their contribution to protein-protein interfaces is shown in Figures 9 and 10. The precision and recall of both SVM and NN show a gradual increase over the sphere radius from 0\AA to 40\AA . This variation can be seen more clearly in the context of the prediction accuracy shown in Figure 10. The SVM approach shows a peak accuracy of about 80% occurring at a radius of 40\AA . NN accuracy also peaks at the same radius. To explore the distribution of data contributing to these predictions, Figure 11 shows the coefficient of variation (the ratio of standard deviation to mean) for each parameter over the radii chosen. Figure 12 shows the impact of isolating the contribution of each parameter to the SVM prediction. Here the microenvironment radius was fixed at 40\AA except for the indicated parameter, which was varied in the range 0\AA to 50\AA .

At lower microenvironment radii, the temperature factor provides the dominant component of the overall accuracy of the predictive model. This covers increasing radii upto about 30\AA . Between 30\AA and 50\AA other parameters,

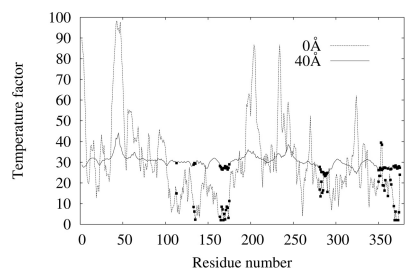


Fig. 5. Residues contributing to the protein-protein interface superimposed on the temperature factor distribution for 1HLU A

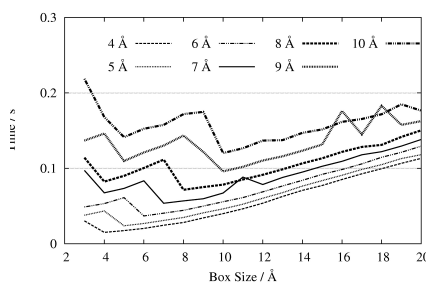


Fig. 7. Effect of cell size on execution time for different sphere radii

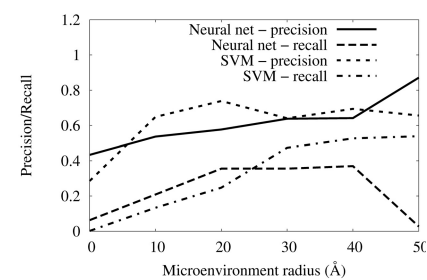


Fig. 9. Precision and recall at varying microenvironment radii

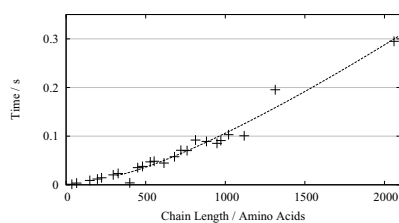


Fig. 6. Summarisation using the 3D grid index

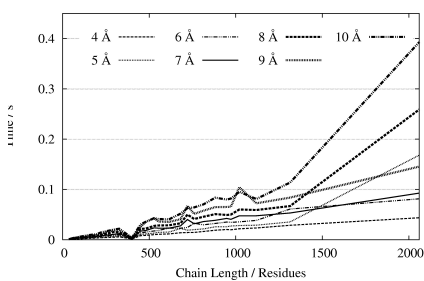


Fig. 8. Index generation at different sphere radii. Cell sizes are set equal to the sphere radius.

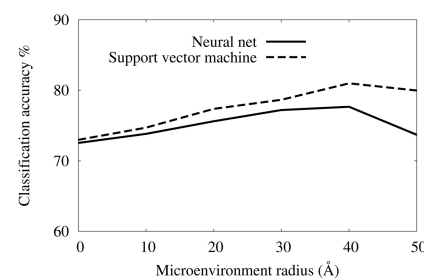


Fig. 10. Accuracy at varying microenvironment radii

particularly hydrophathy play an increasing role in contributing towards the accuracy of the prediction. In all cases however, the use of microenvironments as the basis of generating classifications show evident improvements over the use of data points that do not take into account the neighbourhood surrounding the α -carbon.

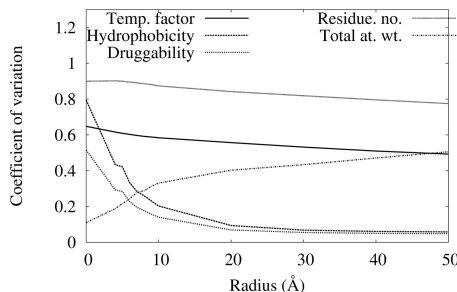


Fig. 11. Coefficients of variation

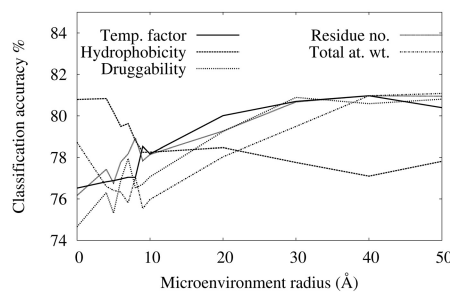


Fig. 12. Principal component analysis

5 Discussion

The experimental work verifies the assumption in constructing spheres in network structures, that the most appropriate cell length matches sphere radius. This result provides confidence in the optimal performance of microenvironment assembly, which is necessary for locating good classifiers within the search space. The on-the-fly approach is efficient enough to remove the necessity for materialising microenvironments. This improves the utility of the method since it removes the need for predicting the combinations of parameters that can distinguish hotspot nodes. If a user interface must respond to a mouse click or a keystroke within 0.1 s, the 3D grid index continues to meet the criteria up to about 1200 residues for the higher sphere sizes and over 2000 residues for sphere sizes of 7\AA and under. This makes it feasible to build a direct manipulation interface to large networks such as those represented by the PDB and provides support for interactive data mining. The experiments show that the performance of the index depends on sphere size, with larger radii making the index less efficient.

Sphere size also has an effect on the use of microenvironments as a basis for classifying hotspots in the network, in this case characterising residues in terms of their contribution to protein-protein interface sites. Microenvironments provide a more effective quantification of the impact of parameter values at a particular site than is available by using localised point values. This effect is visible in predictions based on SVMs and NNs using the same set of parameter values. The benefit of using microenvironments as input into SVMs is significant. The accuracy of the prediction reaches 80% at a sphere radius of 40\AA . This compares favourably with results in the range 60%-73% that are reported in the literature [30,11,35,31]. Using network centrality analysis on residue interaction graphs predicts active sites with a accuracy of 70% [3]. An equivalent effect is noticeable in the precision and recall of SVMs operating on the test set. Precision and recall at 40\AA are 63% and 65% respectively, compared with prior reported equivalent values of 46% and 67% [30]. In this context, neural networks return lower values for precision, recall and accuracy, a point already noted in classifiers developed to address other domains [10].

In the context of network representations of protein structures, the improvement in prediction has the potential for focusing the selection of appropriate sites for targeting drug design aimed at protein-protein interfaces. The longer term consequences are cost reductions during *in vitro* assay. An additional benefit is the potential for scanning a large collection of protein structural data (e.g the Protein Data Bank) with a view to identifying the sites in all the chains where protein-protein interactions may be taking place. Bulk scanning such as this necessitates the development of the optimised indexing approach described in Section 3.

The coefficients of variation suggest that the parameters chosen are subject to considerable variation in microenvironments that range from 0Å to 20Å. Beyond this, hydrophobicity and druggability show less variation. The results reported in Figure 12 suggest that despite restricted variation of these parameters beyond 20Å, they still make an important contribution to the prediction process at microenvironment radii of around 40Å.

This work has focused on the use of 3D coordinates to model protein structures as an example of nodes located within a network. Other approaches to protein modeling include representation as graph structures with edges typically denoting the spatial proximity of atoms within the structure [27]. In this idiom, microenvironments are an appropriate way of characterising the physicochemical topology of proteins because they can be parameterised to span variable sub-graphs within the chain. The utility of this approach is demonstrated in the increased classification accuracy for microenvironment centres. Other applications of graph theory include analysis of social network activity, ecological systems and economic structures [1]. Within such domains, there is considerable challenge in the identification of communities as collections of interconnected nodes [34]. Search methodologies can be deployed to address this problem but they are typically limited in the range of network sizes that can be analysed. Microenvironments are an appropriate tool that can be applied in this context and we are currently developing our approach in this direction.

6 Conclusion

The experimental work reported has evaluated the efficiency of a parameterised 3D grid index for generating microenvironment data for use in the classification of residues in terms of their contribution to protein-protein interface sites. The index was evaluated with protein atomic coordinates and has been shown to be most efficient when the cell size matches the granularity of the summary.

The optimised approach to indexing provides a basis for bulk scanning of protein data to identify sites where protein-protein interactions may occur. The use of microenvironments rather than underlying point data values provides a basis for improving the classification performance of both SVMs and NNs in exploring protein structures. Prediction accuracy increases progressively up to about 80% at a microenvironment radius of around 40Å. The model of node classification based on microenvironments in protein network structures has potential for application in other domains where network size makes conventional analysis infeasible.

References

1. Aggarwal, C.: *Social Network Data Analytics*. Springer (2011)
2. Ahlswede, R., Cai, N.C.N., Li, S.Y.R., Yeung, R.W.: Network information flow (2000)
3. Amitai, G., Shemesh, A., Sitbon, E., Shklar, M., Netanel, D., Venger, I., Pietrokovski, S.: Network analysis of protein structures identifies functional residues. *J. Mol. Biol.* 344(4), 1135–1146 (2004)
4. Ansari, S., Helms, V.: Statistical analysis of predominantly transient protein-protein interfaces. *Proteins* 61, 344–355 (2005)
5. Aurenhammer, F.: Voronoi diagrams—a survey of a fundamental geometric data structure. *ACM Comput. Surv.* 23, 345–405 (1991)
6. Bagley, S., Altman, R.: Characterizing the microenvironment surrounding protein sites. *Protein Science* 4, 622–635 (1995)
7. Bentley, J., Stanat, D., Hollins Williams, E.: The complexity of finding fixed-radius near neighbors. *Information Processing Letters* 6(6), 209–212 (1977)
8. Bentley, J.L.: Multidimensional binary search trees used for associative searching. *Commun. ACM* 18, 509–517 (1975)
9. Berman, H.M., et al.: The Protein Data Bank. *Acta Crystallogr. D* 58(6, pt. 1), 899–907 (2002)
10. Bisbal, J., Engelbrecht, G., Villa-Uriol, M.-C., Frangi, A.F.: Prediction of cerebral aneurysm rupture using hemodynamic, morphologic and clinical features: A data mining approach. In: Hameurlain, A., Liddle, S.W., Schewe, K.-D., Zhou, X. (eds.) *DEXA 2011, Part II. LNCS*, vol. 6861, pp. 59–73. Springer, Heidelberg (2011)
11. Burgoyne, N.J., Jackson, R.M.: Predicting protein interaction sites: binding hot-spots in protein-protein and protein-ligand interfaces. *Bioinformatics* 22(11), 1335–1342 (2006)
12. Foley, C.E., AlAzwari, S., Dufton, M., Wilson, J.N.: Using microenvironments to identify allosteric binding sites. In: *Proc. IEEE International Conference on Bioinformatics and Biomedicine*, pp. 1–5 (2012)
13. Chang, C., Lin, C.: LIBSVM: A library for support vector machines. *ACM TOIST* 2, 27:1–27:27 (2011)
14. Cortes, C., Vapnik, V.: Support-vector networks. *Machine Learning* 20, 273–297 (1995)
15. Csermely, P.: Creative elements: network-based predictions of active centres in proteins and cellular and social networks. *Trends in Biochemical Sciences* 33(12), 569–576 (2008)
16. Ezkurdia, I., Bartoli, L., Fariselli, P., Casadio, R., Valencia, A., Tress, M.L.: Progress and challenges in predicting protein-protein interaction sites. *Briefings in Bioinformatics* 10(3), 233–246 (2009)
17. Fariselli, P., Pazos, F., Valencia, A., Casadio, R.: Prediction of protein-protein interaction sites in heterocomplexes with neural networks. *European Journal of Biochemistry* 269(5), 1356–1361 (2002)
18. Farkas, I.J., Korcsmaros, T., Kovacs, I.A., Mihalik, A., Palotai, R., Simko, G.I., Szalay, K.Z., Szalay-Beko, M., Vellai, T., Wang, S., Csermely, P.: Network-Based Tools for the Identification of Novel Drug Targets. *Sci. Signal.* 4(173), pt. 3+ (2011)
19. Kabsch, W., Sander, C.: Dictionary of protein secondary structure: pattern recognition of hydrogen-bonded and geometrical features. *Biopolymers* 22, 2577–2637 (1983)

20. Kauffman, S.A.: Metabolic stability and epigenesis in randomly constructed genetic nets. *Journal of Theoretical Biology* 22(3), 437–467 (1969)
21. Kirman, A.P.: The economy as an evolving network. *J. Evolutionary Economics* 7(4), 339–353 (1997)
22. Klosowski, J., Held, M., Mitchell, J., Sowizral, H., Zikan, K.: Efficient collision detection using bounding volume hierarchies of k-dops. *IEEE T. Vis. Comput. Gr.* 4(1), 21–36 (1998)
23. Levinthal, C.: Molecular model-building by computer. *Scientific American* 214, 42–52 (1966)
24. Liu, R., Jiang, W., Zhou, Y.: Identifying protein-protein interaction sites in transient complexes with temperature factor, sequence profile & accessible surface area. *Amino Acids* 38(1), 263–270 (2010)
25. MATLAB. version 7.13.0 (R2011b). The MathWorks Inc., Natick, Massachusetts (2011)
26. Shinji, S., Hiroki, S., Kobori, M., Noriaki, H.: Use of amino acid composition to predict ligand-binding sites. *J. Chem. Inf. Model.* 47, 400–406 (2007)
27. Vishveshwara, S., Brinda, K., Kannan, N.: Protein structure: insights from graph theory. *Journal of Theoretical and Computational Chemistry* 1(1), 1–25 (2002)
28. Wood, T., Shenoy, P., Venkataramani, A., Yousif, M.: Sandpiper: Black-box and gray-box resource management for virtual machines. *Computer Networks* 53(17), 2923–2938 (2009)
29. Wu, S., Liu, T., Altman, R.: Identification of recurring protein structure microenvironments and discovery of novel functional sites around cys residues. *BMC Struct. Biol.* 10(4) (2010)
30. Xia, J., Zhao, X., Song, J., Huang, D.: Apis: accurate prediction of hot spots in protein interfaces by combining protrusion index with solvent accessibility. *Bioinformatics* 11(174), 1–14 (2010)
31. Gui, J., Yang, L., Xia, J.F.: Prediction of protein-protein interactions from protein sequence using local descriptors. *Protein Pept. Lett.* 17(9), 1085–1090 (2010)
32. Yuan, Z., Bailey, T.L., Teasdale, R.D.: Prediction of protein B-factor profiles. *Proteins: Struct., Funct., Bioinf.* 58(4), 905–912 (2005)
33. Zhang, G.: Neural networks for classification: A survey. *IEEE Transactions on Systems, Man and Cybernetics - Part C* 30(4), 451–462 (2000)
34. Zhao, Y., Levina, E., Zhu, J.: Community extraction for social networks. *Proc. National Academy of Sciences* 108(18), 7321–7326 (2011)
35. Zhong-Hua, S., Fan, J.: Prediction of protein binding sites using physical and chemical descriptors and the support vector machine regression method. *Chinese Physics B* 19(11), 110502 (2010)